Centrality Dependence of Antiproton Production in Au + Au Collisions

D. Beavis,[1] M. J. Bennett,[2] J. B. Carroll,[3] J. Chiba,[4] A. Chikanian,[2] H. Crawford,[5] M. Cronqvist,[5] Y. Dardenne,[5] R. Debbe,[1] T. Doke,[6] J. Engelage,[5] L. Greiner,[5] T. J. Hallman,[3] R. S. Hayano,[7] H. H. Heckman,[8] T. Kashiwagi,[6] J. Kikuchi,[6] S. Kumar,[2] C. Kuo,[5] P. J. Lindstrom,[8] J. W. Mitchell,[9] S. Nagamiya,[10] J. L. Nagle,[2] J. K. Pope,[2] P. Stankus,[10] K. H. Tanaka,[4] R. C. Welsh,[11] and W. Zhan[10]

(E878 Collaboration)

[1]*Brookhaven National Laboratory, Upton, New York*
[2]*A.W. Wright Nuclear Structure Laboratory, Yale University, New Haven, Connecticut*
[3]*University of California at Los Angeles, Los Angeles, California*
[4]*National Laboratory for High Energy Physics (KEK), Tsukuba, Japan*
[5]*University of California Space Sciences Laboratory, Berkeley, California*
[6]*Waseda University, Tokyo, Japan*
[7]*University of Tokyo, Tokyo, Japan*
[8]*Lawrence Berkeley Laboratory, Berkeley, California*
[9]*Universities Space Sciences Research Association/Goddard Space Flight Center, Greenbelt, Maryland*
[10]*Nevis Laboratory, Columbia University, Irvington, New York*
[11]*Johns Hopkins University, Baltimore, Maryland*

(Received 28 July 1995)

We have measured the yields of antiprotons in Au + Au interactions in the rapidity range $1.2 < y < 2.8$ as a function of centrality using a beam line spectrometer. The shapes of the invariant multiplicity distributions at $p_t = 0$ are used to explore the dynamics of antiproton production and annihilation.

PACS numbers: 25.75.+r

Several experiments have used heavy ion collisions at relativistic energies as a means of creating and studying states of nuclear matter under conditions of extreme temperature and density [1]. It is hoped that in a small fraction of these collisions there will form a new state of strongly interacting matter, the quark-gluon plasma. A proposed signature for the formation of this plasma is the enhanced production of antiprotons and other antibaryons [2]. The enhanced production might be offset by the large probability for antiproton ($\bar{p}$) annihilation in baryon rich environments. At Alternating Gradient Synchrotron (AGS) energies, small impact parameter Au + Au collisions are believed to result in regions that have, for a short time, baryon densities in excess of ten times normal nuclear matter density [3]. Antiprotons may be used as a tool to probe the baryon density in the interaction region if the probability of annihilation in the baryon dense regions is large (as expected in conventional models [4,5]), and also if the annihilation is suppressed in these regions, such as by a third body screening mechanism [6]. Antiproton distributions could also be used to study the dynamics of "resonance matter" [7] and the effects of mean field potentials [8]. The E878 experiment has completed a detailed study of $\bar{p}$ production in Au + Au collisions. We discuss the implications of our data on current notions of how antiprotons are produced and annihilated in high energy heavy ion collisions.

Several other experiments have measured the production of antiprotons using Si beams of momenta 14.6A GeV/c incident on targets of Al, Cu, Au, Pb, and Pt [9–13]. Those $\bar{p}$ yields were consistent with scaling as a simple geometrical factor times the $\bar{p}$ yield in $p + A$ collisions, which could be interpreted in two ways [14]. If $\bar{p}$ production is enhanced, the enhancement is offset by annihilation. Alternatively, if $\bar{p}$ production in Si + A interactions is not enhanced, then $\bar{p}$ annihilation in dense nuclear matter is suppressed. The E802 data [11,12] can also be understood in the context of two cascade models ARC (a Relativistic Cascade, version 1.9.5) [6] and RQMD (Relativistic Quantum Molecular Dynamics, version 1.07, run in the cascade mode) [5] which appear to agree with each other, and with the data. Such is not the case for the much heavier Au + Au system as we show below. In the following, we will describe the first data on $\bar{p}$ production measured as a function of centrality at $p_t \approx 0$ in Au + Au collisions at AGS energies.

The E878 experiment at the Brookhaven National Laboratory Alternating Gradient Synchrotron facility is a zero-degree beam line focusing spectrometer which has a nominal momentum acceptance ($\Delta p/p$) of $\pm 3\%$, and an entrance aperture of solid angle ~ 200 μsr. Particles are identified through measurements of rigidity, charge, and velocity. The spectrometer consists of two sets of dipole magnets, four time-of-flight walls providing charge and velocity information, and two aerogel and two gas Čerenkov detectors to further assist in particle identification. Four sets of drift chambers provide position information along the particle trajectories. The spec-

0031-9007/95/75(20)/3633(4)$06.00

trometer was operated at several rigidities ranging from $+15.0$ GV/c to -20 GV/c. We used a Au target of thickness 0.62 cm (22% of the Au beam interacts with the target). The Au beam fluxes were around 2×10^7 particles per spill. The net integrated beam flux for the data discussed in this Letter was $\sim 3 \times 10^{11}$ particles. The experiment identified $\sim 10^4$ antiprotons with centrality information. The impact parameter, or centrality, of events was determined by an array of Čerenkov detectors. Their performance is discussed in detail elsewhere [15].

Figure 1 shows the time-of-flight spectra of particles detected for a spectrometer rigidity setting of -3.2 GV/c. The data in the lower panel, unlike the data in the upper panel, have a requirement that there be no signals measured in the two gas Čerenkov detectors. It is clear from the plots that we can identify antiprotons easily. The live time fraction for data taking was 80–90%, and our analysis efficiency was ~95%.

Figure 2 shows the invariant multiplicity of antiprotons produced in Au + Au collisions plotted for four nonoverlapping centrality bins. The multiplicity information was used to divide the data into four multiplicity classes: events with multiplicities above the 90% value of the integrated multiplicity distribution (central events), in the range 70–90%, in the range 30–70%, and in the range 0–30%. The measured cross sections are scaled by the appropriate fraction of the total geometric cross section which is assumed to be 6850 mb [16]. The solid points show the measured data and statistical uncertainties. The systematic uncertainties (20%) on the data points are dominated by the accuracy of our knowledge of the beam flux and the acceptance of the apparatus.

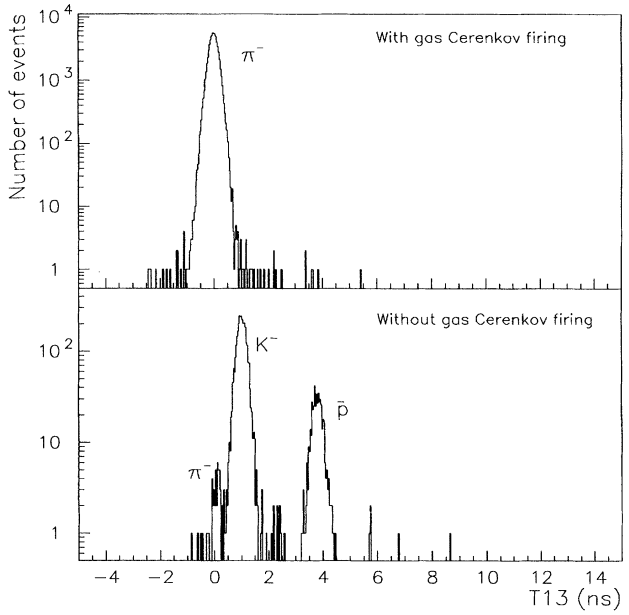

FIG. 1. Particle identification in E878. The top and bottom panels show distributions of the time-of-flight difference between the T1 and T3 detectors with and without the requirement that there be a signal in the Čerenkov detector.

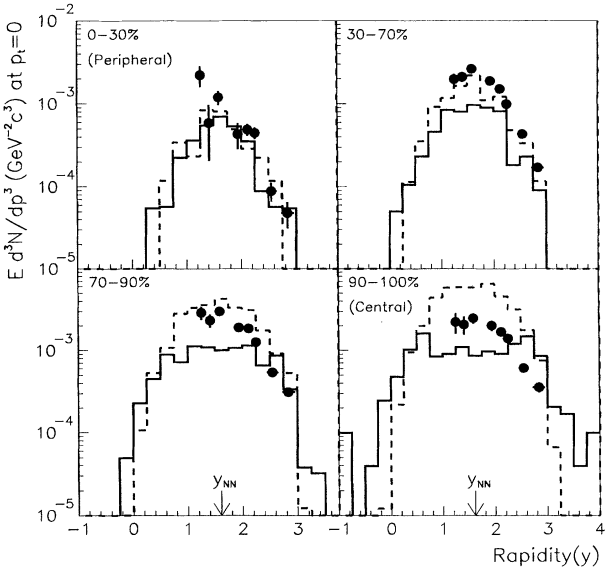

FIG. 2. The invariant multiplicities of antiprotons measured in Au + Au collisions plotted as functions of rapidity for four nonoverlapping centrality bins. The data are shown as symbols, the RQMD calculations as solid lines, and the ARC calculations as dashed lines.

Since particle distributions from Au + Au collisions should be symmetric about the center of mass rapidity $y_{NN} = 1.6$, one can reflect the data about this rapidity. The quality of the reflection gives us a check of the systematic uncertainties in our measurement (see [17] for details). Fitting a Gaussian to the invariant multiplicity data and its reflection allows us to calculate the widths of the distributions for the four centrality bins. One finds that the widths in rapidity σ_y are 0.48 ± 0.04, 0.54 ± 0.03, and 0.57 ± 0.03, 0.62 ± 0.03, for the most peripheral to the most central bins, respectively. The widths of all but the peripheral distribution differ from a simple phase space calculation which predicts $\sigma_y = 0.44$ for antiproton production in $p + p$ collisions at 11A GeV/c [17]. The width of the minimum bias distribution is 0.5 units, and very similar to that measured for impact parameter averaged Si + Au interactions at 14.6A GeV/c [9], in spite of the fact that antiproton production is much closer to threshold at 11A GeV/c. Our minimum bias data are in good agreement with measurements of experiment E886 [13].

In the introduction, we discussed how $\bar{p}$ yields in Si + A collisions scaled with centrality. We can extend such studies to the Au + Au case. We show in Fig. 3 the integrals of the Gaussian fits we described earlier, plotted as a function of the number of first collisions, N_f. First collisions are those in which projectile nucleons are colliding with previously unstruck target nucleons.

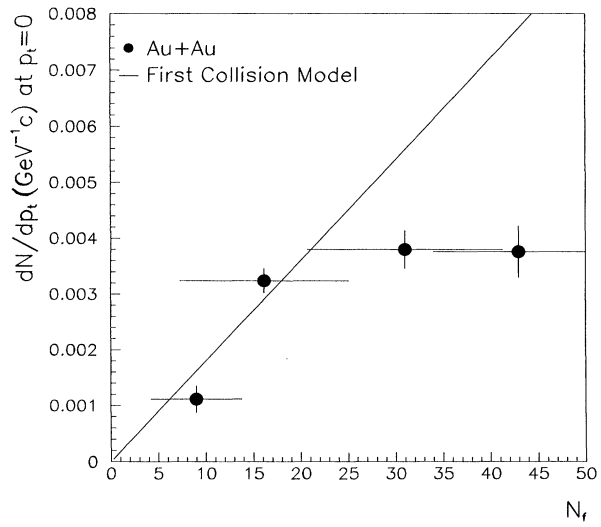

FIG. 3. The integrated yield of antiprotons produced at $p_t \approx 0$ plotted as a function of the number of first collisions.

They are calculated in a Monte Carlo simulation [14] of the nucleus-nucleus collision. N_f is directly related to the geometry of the collision. The horizontal error bars represent the ranges (rms) of N_f contributing to a given centrality bin. The straight line shows a first collisions scaling of a $\bar{p}$ distribution whose shape is determined from a phase space calculation, and whose integral is fixed by the $p + p \rightarrow \bar{p} + \cdots$ cross section predicted by RQMD [17]. The straight line follows the data for peripheral collisions, and deviates significantly in central collisions. Data for Si + A interactions were measured only for $N_f < 15$. Our $\bar{p}$ measurements are consistent with previous observations of linear scaling with N_f at low N_f [10], but show interesting deviations from such scaling at higher N_f.

The heavy ion collision environment differs significantly from that in $p + p$ collisions in that multiple collisions result in the abundant excitation of high-mass baryon resonance states. These can collide with each other and with other baryons to effectively enhance $\bar{p}$ production near and below threshold energies [18]. Resonance production together with hydrodynamic flow and absorption contribute to the changes in the widths of the rapidity distributions of our $\bar{p}$ data. Also shown in Fig. 2 are the $\bar{p}$ predictions of the ARC and RQMD models which include descriptions of the effects mentioned above. They were obtained by making selections on ARC and RQMD events using information obtained from the detailed simulation of our multiplicity detector [15]. Also, to increase statistics, we use versions of both codes that incorporate a factor of 10 enhancement in antinucleon production. Since E878 measures in a small region at $p_t \approx 0$, we select antinucleons from the models if their p_t is less than 200 MeV/c. Note that this is a real cut in p_t, and not a fit to the p_t slope at large p_t followed by an extrapolation to $p_t = 0$.

The two models predict similar $\bar{p}$ abundances for the most peripheral collisions (where the effects of $\bar{p}$ annihilation, and the contributions from resonances are minimal). The big difference between the models comes from the way they describe $\bar{p}$ annihilation. ARC predicts that the antiproton yield increases substantially with centrality. The RQMD model, on the other hand, while successful in describing the yields in peripheral collisions, predicts a significantly different distribution in central collisions. The depletion of antiprotons at midrapidity is a result of the large annihilation that antiprotons are expected to experience in baryon rich environments based on free-space annihilation cross sections. In the ARC model, $\bar{p}$ annihilation is suppressed in high density environments through a third body screening mechanism [6]. Our data for the most central Au + Au collisions lie half way between the two model predictions. The shape of the distributions is suggestive of suppressed $\bar{p}$ annihilation.

There are however other factors that could modify $\bar{p}$ distributions, and which are not implemented in ARC and RQMD. An effect that is small is Coulomb attraction which would produce an enhancement in the abundance of negatively charged secondary particles at $p_t \approx 0$ [19]. The effect is a function of the momentum of the negatively charged particle as well as the number of protons which are close to it in phase space. At $p_t = 0$ we estimate that Coulomb attraction could increase the $\bar{p}$ yield by $<20\%$ near midrapidity and $<5\%$ near beam rapidity, not enough to significantly change the model predictions.

The antiprotons detected in our apparatus could have been produced directly, or through decays of antilambdas. Because of the low Q for the decay $\bar{\Lambda} \rightarrow \bar{p} + \pi^+$, we detect virtually all of the antiprotons produced by antilambdas emitted into our angular acceptance. Preliminary data from the E859 collaboration [20] indicate a $\bar{\Lambda}/\bar{p}$ ratio in central Si + Au collisions to be in excess of unity, suggesting significant differences in $\bar{p}$ and $\bar{\Lambda}$ annihilation. Similar numbers for Au + Au collisions are not available at this time, but could have a large impact on the interpretation of $\bar{p}$ yields. In the ARC model $\bar{\Lambda}$ production is not treated explicitly. The processes leading to $\bar{\Lambda}$ and $\bar{p}$ production and annihilation are assumed effectively to be identical since the $\bar{p}$ abundances are based on a cross section which includes some $\bar{\Lambda} \rightarrow \bar{p}$ decays [6,12]. In RQMD, $\bar{\Lambda}$ production is treated explicitly. The $\bar{\Lambda}/\bar{p}$ ratio is predicted to be ~ 0.4 for minimum bias Au + Au collisions [7]. These antilambdas are not included in the RQMD predictions shown in Fig. 2 and would increase the $\bar{p}$ yield by $<25\%$. The $\bar{\Lambda}$ annihilation in RQMD is similar to that of the $\bar{p}$ since in both cases the annihilation is dominated by a diquark interaction [21].

The implementation of the screening mechanism has been modified in ARC [22]. This increases the $\bar{p}$ annihilation effective cross section and leads to some depletion of

the produced antiprotons, and therefore, better agreement with our data. The RQMD model is able to decrease the deficit of antiprotons seen at y_{NN} in Fig. 2 by taking into account the real part of an antinucleon-nuclear matter optical potential [23]. Since our data test the models only in a small but interesting region of phase space, additional constraints on the scenarios described above could come from $\bar{p}$ measurements made in a larger acceptance spectrometer [24].

E878 has high statistics measurements of antiproton spectra for Au + Au collisions over a wide rapidity range, and with centrality information. Our $\bar{p}$ yields increase linearly with the number of first collisions at low N_f, but fall well below such scaling at high N_f. The ARC and RQMD models which have been successful in the description of p, K, and π data at the AGS, fail to describe our central collisions $\bar{p}$ data. While our data show a clear change in the rapidity distributions in going from peripheral to the most central collisions, this change is significantly smaller than suggested by either of the models investigated. Refinements to the models such as the screening in ARC, and the mean fields in RQMD are both motivated by the existence of high density regions in the collision environment. Our data underscore the importance of the $\bar{p}$ as a probe of the unusual states of matter being created in high energy heavy ion collisions.

We thank the AGS and Tandem staffs for providing the beam. We thank A. Jahns, T. Schlagel, H. Sorge, and C. Spieles for their assistance in providing model predictions and useful insights. This work was supported in part by Grants No. DE-FG02-91ER-40609, No. DE-FG03-88ER-40424, and No. DE-FG03-90ER-40571 with the U.S. Department of Energy.

[1] See articles in *Proceedings of Quark Matter '93* [Nucl. Phys. A **566** (1994)] and *Quark Matter '95* [Nucl. Phys. A (to be published)].

[2] T. DeGrand, Phys. Rev. D **30**, 2001 (1984).

[3] S. H. Kahana, T. J. Schlagel, and Y. Pang, Nucl. Phys. **A566**, 465c (1994).

[4] S. Gavin, M. Gyulassy, M. Plumer, and R. Venugopalan, Phys. Lett. B **234**, 175 (1990).

[5] A. Jahns *et al.*, Phys. Rev. Lett. **68**, 2895 (1992); **72**, 3464 (1994); A. Jahns, Ph.D. thesis, University of Frankfurt, Germany (1995).

[6] S. H. Kahana, Y. Pang, T. Schlagel, and C. B. Dover, Phys. Rev. C **47**, 1356 (1993).

[7] A. Jahns *et al.*, Nucl. Phys. **A566**, 483c (1994).

[8] V. Koch, G. E. Brown, and C. M. Ko, Phys. Lett. B **265**, 29 (1991).

[9] E858 Collaboration, A. Aoki *et al.*, Phys. Rev. Lett. **69**, 2345 (1992).

[10] J. Barrette *et al.*, Phys. Rev. Lett. **70**, 1763 (1993).

[11] T. Abbott *et al.*, Phys. Lett. B **271**, 447 (1992).

[12] T. Abbott *et al.*, Phys. Rev. Lett. **70**, 1393 (1993).

[13] G. Diebold *et al.*, Phys. Rev. C **48**, 2984 (1993).

[14] B. S. Kumar, S. V. Greene, and J. T. Mitchell, Phys. Rev. C **50**, 2152 (1994).

[15] D. Beavis *et al.*, Nucl. Instrum. Methods Phys. Res., Sect. A **357**, 283 (1995).

[16] T. Hoang, B. Cork, and H. Crawford, Z. Phys. C **29**, 611 (1985).

[17] M. Bennett, Ph.D. thesis, Yale University, 1995; E878 Collaboration, D. Beavis *et al.*, Yale Report No. 40609-1148 (to be published).

[18] J. Carroll *et al.*, Phys. Rev. Lett. **62**, 1829 (1989).

[19] E. Shuryak, Nucl. Phys. **A533**, 761 (1991).

[20] See articles by G. S. F. Stephans, and B. A. Cole in Ref. [1].

[21] H. Sorge (private communication).

[22] T. Schlagel *et al.*, in *Proceedings of the 6th Conference on the Intersections of Nuclear and Particle Physics* (AIP, New York, 1995).

[23] C. Spieles *et al.*, University of Frankfurt report, 1995 (to be published).

[24] The BNL-E864 experiment, J. Sandweiss and R. Majka, spokespersons.